A single dose, BCG-adjuvanted COVID-19 vaccine provides sterilizing immunity against SARS-CoV-2 infection in mice

Claudio Counoupas[1,2#], Matt D. Johansen[3#], Alberto O. Stella[4], Duc H. Nguyen[3], Angela L. Ferguson[1,2] Anupriya Aggarwal[4], Nayan D. Bhattacharyya[2], Alice Grey[5], Karishma Patel[6], Rezwan Siddiquee[6], Erica L. Stewart[1], Carl G. Feng[2], Nicole G. Hansbro[3], Umaimainthan Palendira[1], Megan C. Steain[2], Bernadette M. Saunders[3], Jason K. K. Low[6], Joel P. Mackay[6], Anthony D. Kelleher[4], Warwick J. Britton[2,5], Stuart G Turville[4], Philip M. Hansbro[3*], James A. Triccas[1,7*]

[1]School of Medical Sciences, Faculty of Medicine and Health, The University of Sydney, Camperdown, NSW, Australia. [2]Tuberculosis Research Program at the Centenary Institute, The University of Sydney, Sydney, NSW, Australia. [3]Centre for Inflammation, Centenary Institute and University of Technology Sydney, Faculty of Science, School of Life Sciences, Sydney, NSW, Australia. [4]Kirby Institute, University of New South Wales, Sydney, NSW, Australia. [5]Department of Clinical Immunology, Royal Prince Alfred Hospital, Sydney, NSW, Australia. [6]School of Life and Environmental Sciences, The University of Sydney, Sydney, NSW 2006. [7]Charles Perkins Centre and Marie Bashir Institute for Infectious Diseases and Biosecurity, The University of Sydney, Camperdown, NSW, Australia.

[#]Authors contributed equally

*Correspondence to James A. Triccas (jamie.triccas@sydney.edu.au); Philip Hansbro (Philip.Hansbro@uts.edu.au)

ABSTRACT

Global control of COVID-19 requires broadly accessible vaccines that are effective against SARS-CoV-2 variants. In this report, we exploit the immunostimulatory properties of bacille Calmette-Guérin (BCG), the existing tuberculosis vaccine, to deliver a vaccination regimen with potent SARS-CoV-2-specific protective immunity. Combination of BCG with a stabilized, trimeric form of SARS-CoV-2 spike antigen promoted rapid development of virus-specific IgG antibodies in the blood of vaccinated mice, that was further augmented by the addition of alum. This vaccine formulation, BCG:CoVac, induced high-titre SARS-CoV-2 neutralizing antibodies (NAbs) and Th1-biased cytokine release by vaccine-specific T cells, which correlated with the early emergence of T follicular helper cells in local lymph nodes and heightened levels of antigen-specific plasma B cells after vaccination. Vaccination of K18-hACE2 mice with a single dose of BCG:CoVac almost completely abrogated disease after SARS-CoV-2 challenge, with minimal inflammation and no detectable virus in the lungs of infected animals. Boosting BCG:CoVac-primed mice with a heterologous vaccine further increased SARS-CoV-2-specific antibody responses, which effectively neutralized B.1.1.7 and B.1.351 SARS-CoV-2 variants of concern. These findings demonstrate the potential for BCG-based vaccination to protect against major SARS-CoV-2 variants circulating globally.

47 **INTRODUCTION**

48 The world has entered a critical stage in the continuing fight against COVD-19. The
49 deployment of effective vaccines has had a profound impact in reducing cases and SARS-CoV-
50 2 transmission in countries with high vaccine coverage[1,2]. However global cases are again on
51 the rise, driven predominantly by a surge of infections in Europe, South America and the
52 subcontinent due to the emergence of new SARS-CoV-2 variants. Two of the dominant
53 variants of concern (VOCs), B.1.1.7 and B.1.351, both have increased transmissibility[3,4] and
54 antibodies from convalescent patients and vaccinees have a reduced capacity to neutralize
55 B.1.351[5,6]. Vaccination with one of the most widely deployed vaccines, ChAdOx1 nCoV-19,
56 does not protect against mild-to-moderate COVID-19 due to the B.1.351 variant in South
57 Africa[7]. A critical issue is ensuring the adequate supply of vaccines to the hardest-hit low and
58 middle income countries, particularly due to complex logistical requirements (e.g. storage at
59 low temperature for mRNA vaccines). The requirement for multiple doses for most approved
60 vaccines is a barrier to rapid, mass vaccination and has necessitated changes in dosing
61 schedules in some countries to ensure sufficient vaccine coverage[8]. Thus, ensuring the global
62 supply of vaccines effective against emerging variants will be necessary to control the global
63 COVID-19 pandemic.

64 One unique strategy is to 'repurpose' existing licensed vaccines for use against COVID-19.
65 Significant interest has focussed on *Mycobacterium bovis* bacille Calmette-Guerin (BCG), the
66 tuberculosis (TB) vaccine. Considerable data has been accumulated to show that BCG has
67 beneficial, non-specific effects on immunity that affords protection against other pathogens,
68 particularly respiratory infections[9]. Most recently, BCG vaccination was shown to protect
69 against viral respiratory tract infections in the elderly (greater than 65 years old) with no
70 significant adverse events[10]. This non-specific protective effect is attributed to the ability of
71 BCG to induce 'trained immunity' i.e. reprogramming of innate immune responses to provide

72 heterologous protection against disease. For these reasons, a Phase 3, randomised controlled
73 trial in healthcare workers has commenced to determine if BCG vaccination can reduce the
74 incidence and severity of COVID-19 (the BRACE Trial)[9]. While that trial will determine if
75 BCG can reduce the impact on COVID-19 during the current pandemic, BCG does not express
76 SARS-CoV-2 specific antigens and thus, would not induce long-term immune memory.

77 Here, we have exploited the immunostimulatory properties of BCG to develop a SARS-
78 CoV-2 vaccine, BCG:CoVac, that combines a stabilized, trimeric form of the spike protein
79 with the alum adjuvant. BCG:CoVac stimulated SARS-CoV-2-specific antibody and T cell
80 responses in mice after a single vaccination, including the elicitation of high-titre NAbs.
81 Critically, a single dose was shown to protect mice against severe SARS-CoV-2, demonstrating
82 that BCG:CoVac is a highly immunogenic and promising vaccine candidate.

83

84 **RESULTS**

85 **BCG vaccination promotes SARS-CoV-2 specific antibody and T cell**
86 **responses in mice**

87 The immunostimulatory properties of BCG[11] led to us to test if the vaccine could serve as the
88 backbone for a unique vaccine platform against COVID-19. This was also supported by our
89 observation that prior BCG immunization could augment anti-spike IgG responses after
90 boosting with SpK formulated in Alhydrogel/alum (Alm^{SpK}) (Fig. S1). To determine if this
91 property of BCG could be used in a single vaccine formulation, we subcutaneously (s.c)
92 vaccinated mice with a single dose of BCG formulated with a stabilized, trimeric form of the
93 SARS-CoV-2 spike protein[12] and the titre of IgG2c or IgG1 anti-SpK antibodies was
94 determined at various timepoints post-immunization (Fig. 1a). While BCG vaccination resulted
95 in background levels of anti-SpK antibodies, titres were approximately 100-fold higher for both
96 antibody isotypes after BCG^{Spk} vaccination, and similar to those levels achieved with Alm^{SpK}

97 (Fig. 1b, 1c). Addition of alum to BCG^{Spk} (termed BCG:CoVac) further increased antibodies
98 titres, particularly IgG2c, which were significantly greater after BCG:CoVac vaccination
99 compared to mice immunized with either BCG or Alm^{SpK}, at all timepoints examined (Fig. 1b,
100 1c).

101 The IgG2c Ab isotype correlates with Th1-like immunity in C57BL/6 mice[13], and such
102 responses are considered necessary for effective protection against SARS-CoV-2 infection[14].
103 We therefore examined the frequency of IFN-γ-expressing T cells after a single dose of
104 BCG:CoVac at 2 weeks post-vaccination. BCG^{SpK} and BCG:CoVac induced the generation of
105 SpK-specific CD4^{+} and CD8^{+} T cells secreting IFN-γ (Fig. 1d, 1e), consistent with Th1
106 immunity observed after BCG vaccination[15]. The greatest response was observed after
107 vaccination with BCG:CoVac, with the numbers of IFN-γ-secreting T cells significantly
108 increased compared to vaccination with either BCG or Alum^{SpK}. Low levels of the
109 inflammatory cytokines IL-17 and TNF were observed after BCG:CoVac vaccination (Fig. 1e).

110 We further dissected vaccine-induced immunity by defining the cellular composition in
111 draining lymph nodes 7 days after vaccination. Both Alum^{SpK} and BCG:CoVac induced
112 appreciable expansion of SpK-specific germinal centre (GC) B cells
113 (CD19^{+}MHCII^{+}GL7^{+}CD38^{-}; Fig. 2a) and plasma B cells (CD19^{+}MHCII^{+}CD138^{+}; Fig. 2b).
114 Cells with a T follicular helper cell (Tfh) phenotype (CD4^{+}CXCR5^{+}BCL6^{+}) were apparent after
115 vaccination with Alum^{SpK} or BCG:CoVac, with Tfh frequency greatest in the latter group (Fig.
116 2c). The total numbers of GC B cells (Fig. 2d), plasma B cells (Fig. 2e) and Tfh cells (Fig. 2f)
117 were all significantly increased in BCG:CoVac-vaccinated mice compared to immunization
118 with Alum^{SpK}.

119 Overall, these data show that co-delivery of trimeric SpK antigen with BCG vaccination
120 promotes early and pronounced anti-SARS-CoV-2 immunity, and this is further enhanced with
121 the addition of alum.

High-titre, SARS-CoV-2 neutralizing antibodies after a single immunization with BCG:CoVac

The elicitation of GC B cell and Tfh responses after immunization with experimental SARS-CoV-2 vaccines correlate strongly with the induction of neutralizing antibodies (NAbs)[16]. Such NAbs are a key determinant of protection induced by current vaccines used in humans[17]. We therefore measured NAb levels after a single dose of BCG:CoVac. No NAbs were detected in the plasma of mice vaccinated with BCG (Fig. 3a). Surprisingly, NAb titres were at near background levels for mice vaccinated with BCG^{SpK} (Fig. 3a), despite the high levels of IgG Ab isotypes detected in these same animals (Fig. 1). High NAb titres were detected as early as 2 weeks post-immunization upon vaccination with BCG:CoVac, and titres were significantly increased compared to vaccination with $Alum^{SpK}$ (approximate 10-fold increase). The mean NAb titres in the plasma of BCG:CoVac-vaccinated mice were approximately 10-fold greater than those seen in SARS-CoV-2 infected humans (Fig. 3a). Although the levels of NAbs peaked at 2 weeks post-vaccination with BCG:CoVac, they remained significantly elevated up to day 42 post-immunization unlike those in the other immunized groups.

Since previous work suggests that the level of IgG antibody correlates with NAb titres after SARS-CoV-2 infection[18], we examined whether a similar phenomenon was observed after vaccination with BCG:CoVac. Strong correlation ($r > 0.9$) was observed between IgG2c isotype and NAbs in groups vaccinated with BCG:CoVac or $Alum^{SpK}$ (Fig. 3b), with a significant yet less robust correlation between IgG1 and NAbs for these groups (Fig. 3c). There was no correlation between NAbs and either IgG1 or IgG2c Ab for mice vaccinated with BCG^{SpK} alone (Fig. 3d, 3e).

These data suggest that alum is required for the optimal generation of NAbs after BCG:CoVac vaccination. This is a significant advantage for implementation of this vaccine candidate, due to the low cost and long standing safety record of alum[19,20]. Importantly, the

147 potential risk of vaccine-associated enhanced respiratory disease (VAERD) caused by the
148 selective induction of Th2 T cell responses by alum is offset by the strong Th1 immunity
149 induced by BCG:CoVac, which in turn is driven by BCG (Fig. 1e).
150

151 BCG:CoVac affords sterilizing immunity against SARS-CoV-2 infection in 152 K18-hACE2 mice

153 Wild-type mice are not permissive to SARS-CoV-2 infection, owing to incompatibility in the
154 receptor binding domain of the viral spike protein with the murine angiotensin-converting
155 enzyme 2 (ACE2) [21]. Transgenic mice expressing the human (h)ACE2 such as the K18-hACE2
156 mouse, are highly susceptible to SARS-CoV-2 infection, succumbing to lethal infection within
157 7 days post-infection[22]. We therefore assessed the protective role of BCG or BCG:CoVac
158 vaccination in SARS-CoV-2 infection in K18-hACE2 mice. Mice were vaccinated 21 days
159 prior to inoculation with 10^3 PFU SARS-CoV-2 (Fig. 4a). Mice sham vaccinated with PBS
160 succumbed to infection within 6 days with substantial deterioration in their condition with high
161 clinical scores (Fig. 4b) and 20% weight loss (Fig. 4c). This outcome was associated with high
162 viral titres in the airways (bronchoalveolar lavage fluid, BALF) (Fig. 4d) and lung tissues (Fig.
163 4e). These events led to extensive lung inflammation with substantial increases in inflammatory
164 cells in the airways (Fig. 4f) and lung tissue (Fig. 4g), and the levels of the pro-inflammatory
165 cytokine, IL-6, and chemokines KC (murine equivalent of IL-8) and MCP-1, in the lung tissues
166 (Fig. 4h) and airways (Fig. S2). MCP-1 was also increased in serum (Fig. S2). These are the
167 archetypal cytokines associated with severe human COVID-19[23]. Vaccination with BCG
168 showed some beneficial effects and partially protected against weight loss (~10%) and lung
169 IL-6 and KC responses but not in other disease features. Remarkably, vaccination with
170 BCG:CoVac 21 days prior to infection completely protected against infection, with no
171 observable weight loss or any clinical scores throughout the duration of the experiment (Fig.

172 4b, 4c). These mice had no detectable virus in the airways or lungs (Fig. 4D, 4E). They had
173 few signs of lung inflammation with moderate levels on inflammatory cells in the airways and
174 virtually none in the lung tissue (Fig. 4g), and only baseline levels of all pro-inflammatory
175 cytokines in the airways, lung and serum (Fig. 4h, S2). Importantly, combination of the spike
176 protein and alum with BCG did not alter the protective efficacy of the BCG vaccine against
177 aerosol *M. tuberculosis* in mice (Fig 4i).

178 Collectively, these findings demonstrate that single dose administration of BCG:CoVac is
179 sufficient to completely protect mice from the development of COVID-19 disease
180 manifestations, and to neutralize infectious SARS-CoV-2 and prevent pathogenic
181 inflammation in the lung.

182

183 Enhancing BCG:CoVac immunity against SARS-CoV-2 by heterologous 184 vaccine boosting

185 COVID-19 subunit vaccines typically display poor immunity after a single dose and require a
186 booster to induce sufficient generation of NAbs[24]. Whilst we observed high-titre NAbs as early
187 as two weeks post-BCG:CoVac vaccination (Fig. 3), we sought to determine if responses could
188 be further augmented by boosting with a prototype subunit vaccine ($Alum^{SpK}$) (Fig. 5a). At 7
189 days post-boost (day 28), IgG2c titres in plasma from mice primed either with BCG^{SpK} or
190 BCG:CoVac were increased and remained elevated up to day 42 (Fig. 5b). Corresponding
191 augmentation of NAbs was also seen in these boosted groups, with significantly elevated
192 responses in BCG:CoVac primed mice boosted with $Alum^{SpK}$ (Fig. 5c). Boosting $Alum^{SpK}$
193 vaccination with a second dose led to a greater than 10-fold increase in NAbs in boosted mice;
194 however, responses were significantly higher in those with the BCG:CoVac-prime, $Alum^{SpK-}$
195 boost combination (Fig. 5c). Strikingly, plasma from BCG:CoVac-vaccinated mice was able
196 to neutralize both the B.1.1.7 variant (1.3-fold decrease compared to wild-type virus) and

197 B.1.351 variant (2.7-fold decrease) (Fig. 5d). Neutralization capacity against B.1.1.7 and
198 B.1.351 was maintained to some extent after prime-boost with Alum^{SpK} only, however titres
199 were approximately 10-fold less than those following the BCG:CoVac prime, Alum^{SpK}
200 combination (Fig. 5e).

201 Taken together, these data indicate that the antigen-specific immunity imparted by
202 BCG:CoVac can be further enhanced by heterologous boosting with a second SARS-CoV-2
203 vaccine, with this vaccination regime able to induce antibodies that can neutralize key VOCs.

204

205 **DISCUSSION**

206 Global vaccine access and distribution to low- and middle-income countries is critical for the
207 control of the COVID-19 pandemic. Vaccines must offer effective protective immunity yet
208 should be cheap to manufacture and have feasible cold chain management requirements. This
209 study describes a COVID-19 vaccine formulation, BCG:CoVac, that when delivered as a single
210 dose induces potent SARS-CoV-2 specific immunity in mice, particularly the generation of
211 high-titre, anti-viral neutralizing antibodies. Encouragingly, the level of immune responses
212 observed (particularly the generation of neutralizing antibodies) is equivalent to or exceeds
213 immunity elicited by approved COVID-19 vaccines, when these candidate vaccines were tested
214 in the murine model[24-26]. BCG:CoVac may have the additional advantage of inducing
215 protection against other respiratory infections for which BCG is known to induce some level
216 of protective immunity, including future pandemic viruses[11]. In addition, the possibility that
217 prior BCG exposure may impart protection against severe COVID-19[27], which is currently
218 under evaluation through numerous randomised control studies[9], raises the possibility that a
219 BCG-based vaccine could afford protection against SARS-CoV-2 escape mutants or new
220 pandemic coronavirus that may emerge. Indeed our data demonstrate that BCG:CoVac can
221 neutralize two of the key VOCs that are circulating globally, namely B.1.1.7 and B.1351.

222 BCG:CoVac could also provide additional benefit in countries where BCG is part of childhood
223 immunization programs for the control of TB, based on recent findings that repeat BCG
224 vaccination significantly reduced rates of *M. tuberculosis* infection[28].

225 An advantage of our vaccine approach is the use of alum to potentiate immune responses,
226 particularly the generation of NAbs after vaccination. Alum is a low cost, globally accessible
227 vaccine adjuvant with an excellent safety record in humans[19]. The relative paucity of IFN-γ-
228 secreting T cells observed after Alum^{SpK} vaccination corresponds with that previously seen
229 with alum-precipitated vaccines using the spike protein[29] and is consistent with the known
230 preferential priming of Th2-type immunity by alum-based adjuvants[30]. The ability of
231 BCG:CoVac to induce strong Th1 immunity is due to the adjuvant effect of BCG components
232 to induce such responses[31]. This has clear importance, as T cell responses in recovering
233 COVID-19 patients are predominately Th1-driven[32], expression of IFN-γ was lower in severe
234 COVID-19 cases compared to mild ones[33] and the development of Th2 immunity correlated
235 with VAERD[34].We also observed only background levels of the inflammatory cytokines IL-17
236 and TNF after BCG:CoVac delivery, suggesting reduced levels of potentially deleterious,
237 circulating inflammatory cytokines. Heightened expression of IL-17 correlates with severe
238 COVID-19 disease[35], while neutralizing IL-17 has been suggested as a possible therapy to treat
239 acute respiratory distress syndrome in SARS-CoV-2-infected individuals[36]. In addition, the
240 development of VAERD is also associated with Th17 immunity[37].

241 Our study contributes to defining correlates of immunity in animal models that could be
242 applied to fast-track the development of next-generation COVID-19 vaccines. A single dose of
243 BCG:CoVac was sufficient to clear infectious SARS-CoV-2 from the lungs of K18-hACE2
244 mice, with no signs of clinical disease during the infection time-course, which is otherwise
245 lethal (Fig. 4). Our findings are in agreement with previous reports that demonstrate that these
246 mice succumb rapidly to infection, indicating that the level of NAbs elicited by BCG:CoVac

247 is sufficient to clear SARS-CoV-2 infection in this model[21,38]. While NAb levels are known to
248 correlate with efficacy of COVID-9 vaccines in humans[17], other immune parameters may play
249 an important role. Accordingly, we observed that high NAb levels in blood corelated with
250 strong induction of GC and plasma B cells in lymph nodes, as well as heightened levels of Tfh
251 cells. In COVID-19 convalescent individuals, the presence of memory B cells and Tfh are
252 closely associated with NAb activity[38,39]. Further, although BCG vaccination alone did not
253 reduce lung viral load, mice immunized with this vaccine did show an intermediate level of
254 both weight loss and cytokine/chemokine induction during SARS-CoV-2 infection, suggesting
255 a possible 'dampening' of host inflammatory responses (Fig. 4 and Fig. S2). Such an effect
256 was seen in a human challenge model using the live-attenuated yellow fever vaccine, where
257 BCG reduced circulating pro-inflammatory cytokines[40]. It will be of particular interest to see
258 the outcome of ongoing clinical trials to determine if BCG vaccination can reduce COVID-19
259 incidence and severity[9].

260 In conclusion, we describe a COVID-19 vaccine strategy based on the existing BCG
261 vaccine, that would be broadly applicable for all populations susceptible to SARS-CoV-2
262 infection. Of particular note, this strategy could be readily incorporated into current vaccine
263 schedules in countries where BCG is currently used. Further assessment in humans will
264 determine if BCG:CoVac can impart protective immunity against not only SARS-CoV-2, but
265 also other respiratory infections for which BCG has known efficacy.

266

267 # METHODS

268 ## Bacterial culture

269 *M. bovis* BCG (strain Pasteur) was grown at 37°C in Middlebrook 7H9 media (Becton
270 Dickinson, BD, New Jersey, USA) supplemented with 0.5% glycerol, 0.02% Tyloxapol, and
271 10% albumin-dextrose-catalase (ADC) or on solid Middlebrook 7H11 media (BD)

272 supplemented with oleic acid–ADC. To prepare single cell suspensions, cultures in exponential
273 phase (OD_{600}=0.6) were washed in PBS, passaged 10 times through a 27G syringe, briefly
274 sonicated and centrifuged at low speed for 10 min to remove residual bacterial clumps. BCG
275 suspensions were frozen at -80° C in PBS supplemented with 20% glycerol, and colony
276 forming units (CFU) for vaccination enumerated on supplemented Middlebrook 7H11 agar
277 plates.
278

279 **Ethics statement**

280 All mouse experiments were performed according to ethical guidelines as set out by the Sydney
281 Local Health District (SLHD) Animal Ethics and Welfare Committee, which adhere to the
282 Australian Code for the Care and Use of Animals for Scientific Purposes (2013) as set out by
283 the National Health and Medical Research Council of Australia. SARS-CoV-2 mouse infection
284 experiments were approved by the SLHD Institutional Biosafety Committee. COVID-19
285 patients were recruited through Royal Prince Alfred Hospital (RPA) Virtual, a virtual care
286 system enabling remote monitoring of patients. The study protocol was approved by the RPA
287 ethics committee (Human ethics number X20-0117 and 2020/ETH00770) and by the
288 participants' written consent. All associated procedures were performed in accordance with
289 approved guidelines.
290

291 **Immunization**

292 Female C57BL/6 (6-8 weeks of age) purchased from Australian BioResources (Moss Vale,
293 Australia) or hemizygous male K18-hACE2 mice bred in-house[41] were housed at the Centenary
294 Institute in specific pathogen-free conditions. SARS-CoV-2 full-length spike stabilized,
295 trimeric protein (SpK) was expressed in EXPI293F™ cells and purified as described
296 previously[42]. Mice (n=3-4) were vaccinated subcutaneously in the footpad (s.c) with $5x10^5$

297 CFU of BCG alone, 5 μg of SpK combined with either BCG (BCG^{SpK}) or 100 μg of Alhydrogel
298 (Alum) (Invivogen, California, USA, $Alum^{SpK}$), or a combination of BCG ($5x10^5$ CFU), SpK
299 (5 μg) and Alyhydrogel (100 μg) (BCG:CoVac). Some mice were boosted three weeks after
300 the first vaccination with 5 μg of SpK combined with 100 μg of Alhyhdrogel. Mice were bled
301 fortnightly after the first immunization (collected in 10 μl of Heparin 50000 U/ml). Plasma was
302 collected after centrifugation at 300 x *g* for 10 min and remaining blood was resuspended in 1
303 mL of PBS Heparin 20 U/mL, stratified on top of Histopaque 10831 (Sigma-Aldrich, Missouri,
304 USA) and the PBMC layer collected after gradient centrifugation.
305

306 **Flow cytometry assays**

307 Popliteal lymph nodes were collected at day 7 post immunization, and single cell suspensions
308 were prepared by passing them through a 70 μm sieve. To assess specific B cell responses,
309 $2x10^6$ cells were surface stained with Fixable Blue Dead Cell Stain (Life Technologies) and
310 Spike-AF647 (1 μg), rat anti-mouse GL7-AF488 (clone GL7, 1:200, Biolegend cat#144612),
311 rat anti-mouse MHC-II-AF700 (clone M5/114.15.2, 1:150, cat#107622), rat anti-mouse IgD-
312 PerCP5.5 (clone 11-26c.2a, 1:200, BD, cat#564273), rat anti-mouse IgM-BV421 (clone
313 RMM-1, 1:200, Biolegend, cat#406518), rat anti-mouse CD138-BV605 (clone 281-2, 1:200,
314 Biolegend, cat#142516), rat anti-mouse CD19-BV785 (clone 1D3, 1:200, BD, cat#563333),
315 rat anti-mouse CD38-APCy7 (clone 90, 1:200, Biolegend, cat#102728). To assess T cell
316 responses, $2x10^6$ lymph node cells were stained with the following monoclonal antibodies: rat
317 anti-mouse CXCR5-biotin (clone 2G8, 1:100, BD, cat#551960), streptavidin PECy7, rat anti-
318 mouse CD4-AF700 (clone RM4-5, 1:200, BD cat#557956), rat anti-mouse CD8-APCy7 (clone
319 53-6.7, 1:200, BD cat#557654), rat anti-mouse CD44-BV605 (clone IM7, 1:300, BD
320 cat#563058). Cells were then fixed and permeabilized using the eBioscience
321 fixation/permeabilization kit (ThermoFischer) according to the manufacturer's protocol and

322 intracellular staining was performed using anti-BCL-6-AF647 (clone K112-91, 1:100, BD,
323 cat#561525).
324 To assess SpK-specific cytokine induction by T cells, murine PBMCs were stimulated for
325 4 hrs with SpK (5 μg/mL) and then supplemented with Protein Transport Inhibitor cocktail
326 (Life Technologies, California, USA) for a further 10-12 hrs. Cells were surface stained with
327 Fixable Blue Dead Cell Stain (Life Technologies) and the marker-specific fluorochrome-
328 labeled antibodies rat anti-mouse CD4-AF700 (clone RM4-5, 1:200, BD cat#557956), rat anti-
329 mouse CD8-APCy7 (clone 53-6.7, 1:200, BD cat#557654), rat anti-mouse CD44-FITC (clone
330 IM7, 1:300, BD cat#561859). Cells were then fixed and permeabilized using the BD
331 Cytofix/Cytoperm™ kit according to the manufacturer's protocol. Intracellular staining was
332 performed using rat anti-mouse IFN-γ-PECy7 (clone XMG1-2, 1:300, BD cat#557649), rat
333 anti-mouse IL-2-PE (clone JES6-5H4, 1:200, BD cat#554428), rat anti-mouse IL-17-PB (clone
334 TC11-18H10.1, 1:200, cat#506918, BioLegend California, USA), rat anti-mouse TNF-
335 PErCPCy5.5 (clone MP6-XT22, 1:200, BD cat#560659). All samples were acquired on a BD
336 LSR-Fortessa (BD) or a BD-LSRII and assessed using FlowJo™ analysis software v10.6
337 (Treestar, USA).
338

339 **Antibody ELISA**

340 Microtitration plates (Corning, New York, USA) were incubated overnight with 1 μg/mL SpK
341 at room temperature (RT), blocked with 3% BSA and serially diluted plasma samples were
342 added for 1 hour at 37˚C. Plates were washed and biotinylated polyclonal goat anti-mouse IgG1
343 (1:50,000, abcam Cambridge, UK, cat#ab97238), polyclonal goat anti-mouse IgG2c (1:10,000,
344 Abcam, cat# ab97253), or polyclonal goat anti-mouse IgG (1:350,000, clone abcam
345 cat#ab6788) added for 1 hour at RT. After incubation with streptavidin-HRP (1:30,000, abcam,
346 cat#405210) for 30 min at RT, binding was visualized by addition of tetramethyl benzene

347 (Sigma-Aldrich). The reaction was stopped with the addition of 2N H_2SO_4 and absorbances
348 were measured at 450 nm using a M1000 pro plate reader (Tecan, Männedorf, Switzerland).
349 End point titres were calculated as the dilution of the sample that reached the average of the
350 control serum ± 3 standard deviations.
351

352 **High content live SARS-CoV-2 neutralization assay**

353 High-content fluorescence microscopy was used to assess the ability of sera/plasma to inhibit
354 SARS-CoV-2 infection and the resulting cytopathic effect in live permissive cells (VeroE6).
355 Sera were serially diluted and mixed in duplicate with an equal volume of $1.5x10^3$ $TCID_{50}$/mL
356 virus solution (B.1.319) or $1.25x10^4$ $TCID_{50}$/mL virus solution (A2.2, B.1.1.7, B.1.351). After
357 1 hour of virus-serum coincubation at 37°C, 40 µL were added to equal volume of freshly-
358 trypsinised VeroE6 cells in 384-well plates ($5x10^3$/well). After 72 hrs, cells were stained with
359 NucBlue (Invitrogen, USA) and the entire well surface was imaged with InCell Analyzer 2500
360 (Cytiva). Nuclei counts were obtained for each well with InCarta software (Cytiva), as proxy
361 for cell death and cytopathic effect resulting from viral infection. Counts were compared
362 between convalescent sera, mock controls (defined as 100% neutralization), and infected
363 controls (defined as 0% neutralization) using the formula; % viral neutralization = (D-(1-
364 Q))x100/D, where Q = nuclei count of sample normalized to mock controls, and D = 1-Q for
365 average of infection controls. The cut-off for determining the neutralization endpoint titre of
366 diluted serum samples was set to ≥50% neutralization.
367

368 **SARS-CoV-2 challenge experiments**

369 Male hemizygous K18-hACE2 mice were transported to the PC3 facility in the Centenary
370 Institute for SARS-CoV-2 infection. Mice were anaesthetised with isoflurane followed by
371 intranasal challenge with 10^3 PFU SARS-CoV-2 (VIC01/2020) in a 30 µL volume. Following

372 infection, mice were housed in the IsoCage N biocontainment system (Tecniplast, Italy) and
373 were given access to standard rodent chow and water *ad libitum*. Mice were weighed and
374 monitored daily, with increased frequency of monitoring when mice developed symptoms. At
375 day 6 post-infection, mice were euthanised with intraperitoneal overdose of pentobarbitone
376 (Virbac, Australia). Blood was collected *via* heart bleed, allowed to coagulate at RT and
377 centrifuged (10,000 *g*, 10 min) to collect serum. Multi-lobe lungs were tied off and BALF was
378 collected from the single lobe *via* lung lavage with 1 mL HANKS solution using a blunted 19-
379 gauge needle inserted into the trachea. BALF was centrifuged (300 *g*, 4°C, 7 min), and
380 supernatants collected and snap frozen. Cell pellets were treated with 200 µL Red Blood Cell
381 Lysis Buffer (ThermoFisher, USA) for 5 min, followed by addition of 700 µL HANKS solution
382 to inactivate the reaction and then centrifuged again. Cell pellets were resuspended in 160 µL
383 HANKS solution and enumerated using a haemocytometer (Sigma-Aldrich, USA). Multi-lobe
384 lungs were collected and cut into equal thirds, before snap freezing on dry ice. Lung
385 homogenates were prepared fresh, with multi-lobe lungs placed into a gentleMACS C-tube
386 (Miltenyi Biotec, Australia) containing 2 mL HANKS solution. Tissue was homogenised using
387 a gentleMACS tissue homogeniser, after which homogenates were centrifuged (300 *g*, 7 min)
388 to pellet cells, followed by collection of supernatants for plaque assays and cytokine/chemokine
389 measurements. The single lobe lung was perfused with 0.9% NaCl solution *via* the heart,
390 followed by inflation with 0.5 mL 10% neutral buffered formalin through the trachea, and
391 placed into a tube containing 10% neutral buffered formalin. Following fixation for at least 2
392 weeks, single lobes were transported to a PC2 facility where they were paraffin-embedded,
393 sections cut to 3 µm thickness using a Leica microtome (Leica, Germany) and then stained
394 using Quick Dip Stain Kit (Modified Giemsa Stain) protocol as per manufacturer's instructions
395 (POCD Scientific, Australia). Inflammatory cells in single lobe lungs were counted using a
396 Zeiss Axio Imager.Z2 microscope with a 40X objective (Zeiss, Germany).

397 **Plaque assays**

398 VeroE6 cells (CellBank Australia, Australia) were grown in Dulbecco's Modified Eagles
399 Medium (Gibco, USA) supplemented with 10% heat-inactivated foetal bovine serum (Sigma-
400 Aldrich, USA) at 37°C/5% CO_2. For plaque assays, cells were placed into a 24-well plate at
401 $1.5x10^5$ cells/well and allowed to adhere overnight. The following day, virus-containing
402 samples were serially diluted in Modified Eagles Medium (MEM), cell culture supernatants
403 removed from the VeroE6 cells and 250 µL of virus-containing samples was added to cell
404 monolayers. Plates were incubated and gently rocked every 15 min to facilitate viral adhesion.
405 After 1 hr, 250 µL of 0.6% agar/MEM solution was gently overlaid onto samples and placed
406 back into the incubator. At 72 hrs post-infection, each well was fixed with an equal volume of
407 8% paraformaldehyde solution (4% final solution) for 30 min at RT, followed by several
408 washes with PBS and incubation with 0.025% crystal violet solution for 5 min at RT to reveal
409 viral plaques.

410

411 **Cytometric bead arrays (CBAs)**

412 CBAs were performed as per the manufacturer's instructions (Becton Dickinson, USA).
413 Briefly, a standard curve for each analyte was generated using a known standard supplied with
414 each CBA Flex kit. For each sample, 10 µL was added to a well in a 96-well plate, followed
415 by incubation with 1 µL of capture bead for each analyte (1 hr, RT, in the dark). Following
416 capture, 1 µL of detection bead for each analyte was added to each well, followed by incubation
417 (2 hrs, RT, in the dark). Samples were then fixed overnight in an equal volume of 8%
418 paraformaldehyde solution (4% final solution). The following day, samples were transferred to
419 a new 96-well plate and then transported to the PC2 facility for a second round of fixation.
420 Samples were examined using a BD LSR Fortessa equipped with a High-Throughput Sampler
421 (HTS) plate reader.

422 ## *Mycobacterium tuberculosis* aerosol challenge

423 Eight weeks after the last vaccination mice were infected with *M. tuberculosis* H37Rv via the
424 aerosol route using a Middlebrook airborne infection apparatus (Glas-Col, IN, USA) with an
425 infective dose of ~100 viable bacilli. Four weeks later, the lungs and spleen were harvested,
426 homogenized, and plated after serial dilution on supplemented Middlebrook 7H11 agar plates.
427 Colonies forming units (CFU) were determined 3 weeks later and expressed as $\log_{10}$ CFU.

428

429 ## Statistical analysis

430 The significance of differences between experimental groups was evaluated by one-way
431 analysis of variance (ANOVA), with pairwise comparison of multi-grouped data sets achieved
432 using Tukey's or Dunnett's *post-hoc* test. Differences were considered statistically significant
433 when $p \leq 0.05$.

434

435 ## ACKNOWLEDGMENTS

436 This work was supported by MRFF COVID-19 Vaccine Candidate Research Grant 2007221
437 (JAT, CC, PMH, SGT, MCG, ALF, WJB). We thank Florian Krammer of the Icahn School of
438 Medicine, Mt Sinai for provision of the pCAGGS vector containing the SARS-CoV-2 Wuhan-
439 Hu-1 Spike Glycoprotein Gene. We acknowledge the support of the University of Sydney
440 Advanced Cytometry Facility and the animal facility at the Centenary Institute. We thank Sunil
441 David (ViroVax LLC) and Wolfgang Leitner (NIAID, NIH) for helpful discussions. PMH is
442 funded by a Fellowship and grants from the National Health and Medical Research Council
443 (NHMRC) of Australia (1175134) and by UTS. JAT, BMS and WJB are supported by the
444 NHMRC Centre of Research Excellence in Tuberculosis Control (1153493). The establishment
445 of the PC3 COVID-19 facility was supported by UTS and the Rainbow Foundation.

446

447 **AUTHOR CONTRIBUTIONS**

448 CC, MDJ, AOS, SGT, PHM and JAT designed the study. CC, MDJ, AOS, DHN, ALF, AA,
449 RS, NDB, AG, KP, BMS, JKKL, SGT performed the experiments. All authors contributed to
450 data analysis/interpretation. CC, MDJ, PHM and JAT wrote the first manuscript draft and all
451 authors provided revision to the scientific content of the final manuscript.

452

453 **REFERENCES**

454

455 1 Dagan, N. *et al.* BNT162b2 mRNA Covid-19 Vaccine in a Nationwide Mass Vaccination

456 Setting. *N Engl J Med* **384**, 1412-1423 (2021).

457 2 Pritchard, E. *et al.* Impact of vaccination on SARS-CoV-2 cases in the community: a

458 population-based study using the UK's COVID-19 Infection Survey. *medRxiv* (2021).

459 3 Davies, N. G. *et al.* Increased mortality in community-tested cases of SARS-CoV-2

460 lineage B.1.1.7. *Nature* (2021).

461 4 Tegally, H. *et al.* Detection of a SARS-CoV-2 variant of concern in South Africa. *Nature*

462 **592**, 438-443 (2021).

463 5 Wang, P. *et al.* Antibody resistance of SARS-CoV-2 variants B.1.351 and B.1.1.7. *Nature*

464 **593**, 130-135 (2021).

465 6 Wibmer, C. K. *et al.* SARS-CoV-2 501Y.V2 escapes neutralization by South African

466 COVID-19 donor plasma. *Nat Med* **27**, 622-625 (2021).

467 7 Madhi, S. A. *et al.* Efficacy of the ChAdOx1 nCoV-19 Covid-19 Vaccine against the

468 B.1.351 Variant. *N Engl J Med* **384**, 1885-1898 (2021).

469 8 Iacobucci, G. & Mahase, E. Covid-19 vaccination: What's the evidence for extending the

470 dosing interval? *BMJ* **372** (2021).

471 9 Netea, M. G. *et al.* Trained Immunity: a Tool for Reducing Susceptibility to and the

472 Severity of SARS-CoV-2 Infection. *Cell* **181**, 969-977 (2020).

473 10 Giamarellos-Bourboulis, E. J. *et al.* Activate: Randomized Clinical Trial of BCG

474 Vaccination against Infection in the Elderly. *Cell* **183**, 315-323 e319 (2020).

475 11 Covian, C. *et al.* BCG-Induced Cross-Protection and Development of Trained Immunity:

476 Implication for Vaccine Design. *Front Immunol* **10**, 2806 (2019).

477 12 Amanat, F. *et al.* A serological assay to detect SARS-CoV-2 seroconversion in humans.

478 Nature Medicine **26**, 1033-1036 (2020).

479 13 Nazeri, S., Zakeri, S., Mehrizi, A. A., Sardari, S. & Djadid, N. D. Measuring of IgG2c
480 isotype instead of IgG2a in immunized C57BL/6 mice with *Plasmodium vivax* TRAP as a
481 subunit vaccine candidate in order to correct interpretation of Th1 versus Th2 immune
482 response. *Exp Parasitol* **216**, 107944 (2020).
483 14 Sauer, K. & Harris, T. An Effective COVID-19 Vaccine Needs to Engage T Cells. *Front*
484 *Immunol* **11**, 581807 (2020).
485 15 Counoupas, C. & Triccas, J. A. The generation of T-cell memory to protect against
486 tuberculosis. *Immunol Cell Biol* **97** (2019).
487 16 Lederer, K. *et al.* SARS-CoV-2 mRNA Vaccines Foster Potent Antigen-Specific Germinal
488 Center Responses Associated with Neutralizing Antibody Generation. *Immunity* **53**, 1281-
489 1295 e1285 (2020).
490 17 Khoury, D. S. *et al.* Neutralizing antibody levels are highly predictive of immune
491 protection from symptomatic SARS-CoV-2 infection. *Nature Medicine* (2021).
492 18 Suthar, M. S. *et al.* Rapid Generation of Neutralizing Antibody Responses in COVID-19
493 Patients. *Cell Rep Med* **1**, 100040 (2020).
494 19 Hotez, P. J., Corry, D. B., Strych, U. & Bottazzi, M. E. COVID-19 vaccines: neutralizing
495 antibodies and the alum advantage. *Nat Rev Immunol* **20**, 399-400 (2020).
496 20 Lancet Covid-19 Commissioners, T. F. C. & Commission, S. Lancet COVID-19
497 Commission Statement on the occasion of the 75th session of the UN General Assembly.
498 *Lancet* **396**, 1102-1124 (2020).
499 21 Johansen, M. D. *et al.* Animal and translational models of SARS-CoV-2 infection and
500 COVID-19. *Mucosal Immunol* **13**, 877-891 (2020).
501 22 Winkler, E. S. *et al.* SARS-CoV-2 infection of human ACE2-transgenic mice causes
502 severe lung inflammation and impaired function. *Nat Immunol* **21**, 1327-1335 (2020).

503 23 Yang, Y. *et al.* Plasma IP-10 and MCP-3 levels are highly associated with disease severity
504 and predict the progression of COVID-19. *J Allergy Clin Immunol* **146**, 119-127 e114
505 (2020).
506 24 J.-H. Tian *et al.* SARS-CoV-2 spike glycoprotein vaccine candidate NVX-CoV2373
507 immunogenicity in baboons and protection in mice *Nat Commun* ***12,*** 372 (2021).
508 25 Corbett, K. S. *et al.* SARS-CoV-2 mRNA vaccine design enabled by prototype pathogen
509 preparedness. *Nature* **586**, 567-571 (2020).
510 26 Graham, S. P. *et al.* Evaluation of the immunogenicity of prime-boost vaccination with the
511 replication-deficient viral vectored COVID-19 vaccine candidate ChAdOx1 nCoV-19.
512 *NPJ Vaccines* **5**, 69 (2020).
513 27 Escobar, L. E., Molina-Cruz, A. & Barillas-Mury, C. BCG vaccine protection from severe
514 coronavirus disease 2019 (COVID-19). *Proc Natl Acad Sci U S A* **117**, 17720-17726
515 (2020).
516 28 Nemes, E. *et al.* Prevention of *M. tuberculosis* Infection with H4:IC31 Vaccine or BCG
517 Revaccination. *N Engl J Med* **379**, 138-149 (2018).
518 29 Kuo, T. Y. *et al.* Development of CpG-adjuvanted stable prefusion SARS-CoV-2 spike
519 antigen as a subunit vaccine against COVID-19. *Sci Rep* **10**, 20085 (2020).
520 30 HogenEsch, H., O'Hagan, D. T. & Fox, C. B. Optimizing the utilization of aluminum
521 adjuvants in vaccines: you might just get what you want. *NPJ Vaccines* **3**, 51 (2018).
522 31 Uthayakumar, D. *et al.* Non-specific Effects of Vaccines Illustrated Through the BCG
523 Example: From Observations to Demonstrations. *Front Immunol* **9**, 2869 (2018).
524 32 Grifoni, A. *et al.* Targets of T Cell Responses to SARS-CoV-2 Coronavirus in Humans
525 with COVID-19 Disease and Unexposed Individuals. *Cell* **181**, 1489-1501 e1415 (2020).
526 33 Chen, G. *et al.* Clinical and immunological features of severe and moderate coronavirus
527 disease 2019. *J Clin Invest* **130**, 2620-2629 (2020).

528 34 Jeyanathan, M. *et al.* Immunological considerations for COVID-19 vaccine strategies. *Nat*
529 *Rev Immunol* **20**, 615-632 (2020).
530 35 Xu, Z. *et al.* Pathological findings of COVID-19 associated with acute respiratory distress
531 syndrome. *Lancet Respir Med* **8**, 420-422 (2020).
532 36 Pacha, O., Sallman, M. A. & Evans, S. E. COVID-19: a case for inhibiting IL-17? *Nat Rev*
533 *Immunol* **20**, 345-346 (2020).
534 37 Hotez, P. J., Corry, D. B. & Bottazzi, M. E. COVID-19 vaccine design: the Janus face of
535 immune enhancement. *Nat Rev Immunol* **20**, 347-348 (2020).
536 38 Zheng, J. *et al.* COVID-19 treatments and pathogenesis including anosmia in K18-hACE2
537 mice. *Nature* **589**, 603-607 (2021).
538 39 Wheatley, A. K. *et al.* Evolution of immune responses to SARS-CoV-2 in mild-moderate
539 COVID-19. *Nat Commun* **12**, 1162 (2021).
540 40 Arts, R. J. W. *et al.* BCG Vaccination Protects against Experimental Viral Infection in
541 Humans through the Induction of Cytokines Associated with Trained Immunity. *Cell Host*
542 *Microbe* **23**, 89-100 e105 (2018).
543 41 McCray, P. B., Jr. *et al.* Lethal infection of K18-hACE2 mice infected with severe acute
544 respiratory syndrome coronavirus. *J Virol* **81**, 813-821 (2007).
545 42 Xi, C. R. *et al.* A Novel Purification Procedure for Active Recombinant Human DPP4 and
546 the Inability of DPP4 to Bind SARS-CoV-2. *Molecules* **25** (2020).
547
548

549 # FIGURE LEGENDS

550 **Fig. 1 | Single immunization with BCG:CoVac vaccine induces rapid development of anti-**
551 **SARS-CoV-2 spike antibodies and IFN-γ-secreting T cells. a**, C57BL/6 mice were
552 vaccinated subcutaneously with PBS, BCG, BCG^{SpK}, $Alum^{SpK}$ or BCG:CoVac and whole
553 blood collected at day 14, 28 and 42. **b**,**c**, Spike-specific IgG1 and IgG2c titres in plasma were
554 determined by ELISA and estimated by the sigmoidal curve of each sample interpolated with
555 the threshold of the negative sample ± 3 standard deviations. The dotted line shows the limit
556 of detection. **d**, At 14 days post-vaccination PBMCs were restimulated *ex vivo* with 5 μg/mL
557 of SARS-CoV-2 spike and cytokine production determined by flow cytometry. Representative
558 dot plots of $CD44^+$ $CD4^+$ T cells and $CD44^+$ $CD8^+$ T cells expressing IFN-γ. **e**, Numbers of
559 circulating $CD4^+$ and $CD8^+$ T cells expressing IFN-γ or $CD4^+$ T cells expressing IL-17 or TNF.
560 Data presented as mean ± s.d. Significant differences between groups compared to BCG^{Spk}
561 *p<0.05, **p<0.01, ***p<0.01 or $Alum^{Spk}$ †p<0.05, ††p<0.01, †††p<0.001 were determined
562 using one-way ANOVA.

563

564 **Fig. 2 | BCG:CoVac vaccination promotes expansion of T follicular helper cells and spike-**
565 **specific B cells in mice. a-c**, C57BL/6 mice were vaccinated subcutaneously with PBS, BCG,
566 BCG^{SpK}, $Alum^{SpK}$ or BCG:CoVac and 7 days after immunization B and T cell response
567 assessed by multicolour flow cytometry in the draining lymph node. Shown are representative
568 dot plots of spike-specific germinal centre B cells (**a**, $CD19^+MHCII^+GL7^+CD38^-$), plasma B
569 cells (**b**, $CD19^+MHCII^+CD138^+$) and T follicular helper T cells (**c**, $CXCR5^+BCL6^+$). **d-f**, The
570 total number of **d**, $spike^+$ GC B cells, **e**, $spike^+$ plasma cells and **f**, T follicular helper cells. Data
571 presented as mean ± s.d. Significant differences between groups *p<0.05, **p<0.01,
572 ***p<0.01 were determined by one-way ANOVA.

573

574 **Fig. 3 | BCG:CoVac induces high titre neutralizing antibodies against live SARS-CoV-2**
575 **that correlate with the production of antigen-specific IgG2c. a-e**, Plasma from vaccinated
576 mice (from Fig. 1) were tested for neutralizing activity against live SARS-CoV-2 infection of
577 VeroE6 cells. **a**, Neutralizing antibody (NAb) titres (IC_{50}) were calculated as the highest
578 dilution of plasma that still retained at least 50% inhibition of infection compared to controls.
579 NAb titres from PCR confirmed SARS-CoV-2-infected individuals (COVID) were determined
580 using the same method. **b**,**c**, Spearman correlations of spike-specific IgG2c or IgG1 titres and
581 NAbs after $Alum^{SpK}$ or BCG:CoVac vaccination. **d**,**e**, Correlation of IgG2c or IgG1 titres and
582 NAbs after vaccination with BCG^{SpK}. The dotted line shows the limit of detection. Data
583 presented as mean ± s.d. Significant differences between groups compared to BCG^{Spk}
584 **p<0.01, ***p<0.0 or $Alum^{Spk}$ †p<0.05, †††p<0.001 was determined by one-way ANOVA.
585
586 **Fig. 4 | A single dose of BCG:CoVac protects against severe SARS-CoV-2 infection. a**,
587 Mice were immunized with sham (PBS), BCG or BCG:CoVac 21 days prior to challenge with
588 10^3 PFU SARS-CoV-2. Disease outcomes were assessed 6 days later. **b**, Clinical scores at day
589 6 post-infection. **c**, Percentage of initial body weight loss in hemizygous male K18-hACE2
590 mice (n=4/group). Viral titres in lung homogenates (**d**) or bronchoalveolar lavage fluid
591 (BALF) (**e**) were determined using plaque assay. The dotted line represents the limit of
592 detection. **f**, Total inflammatory cells in bronchoalveolar lavage fluid (BALF). **g**, Total number
593 of inflammatory cells in stained histological sections of lungs. **h**, Cytokine/chemokine
594 quantification in lung homogenates. **i**, Six weeks after immunization mice were challenged
595 with *M. tuberculosis* H37Rv by aerosol (~100 CFU) and four weeks later the bacterial load
596 was assessed in the lungs and presented as log_{10} of the mean CFU ± SEM. Significant
597 differences between groups *p<0.05, **p<0.01 were determined by one-way ANOVA.
598

599 **Fig. 5 | Heterologous boosting of BCG:CoVac-primed mice results in augmented SARS-**
600 **CoV-2-specific IgG2c titres and neutralizing antibodies. a**, C57BL/6 mice were vaccinated
601 (as in Fig. 1) and at day 21 mice were boosted with $Alum^{Spk}$. **b**, Spike-specific IgG2c titres in
602 plasma were determined by ELISA estimated from the sigmoidal curve of each sample
603 interpolated with the threshold of the negative sample ± 3 standard deviations. **c**, Neutralizing
604 antibody (NAb) titres (IC_{50}) were calculated as the highest dilution of plasma for all groups
605 that still retained at least 50% inhibition of infection compared to controls. The dotted line
606 shows the limit of detection. **d**,**e**, NAb titres against the B.1.1.7 or B.1.351 SARS-CoV-2
607 variants were also determined using plasma from either **d**, $Alum^{SpK}$ or **e**, BCG:CoVac-
608 vaccinated mice. Data presented as mean ± s.d. Significant differences between groups
609 compared to BCG^{Spk} *p<0.05, **p<0.01, ***p<0.01 or $Alum^{Spk}$ †p<0.05, ††p<0.01,
610 †††p<0.001 were determined by one-way ANOVA.
611
612
613
614
615
616
617

Figure 1

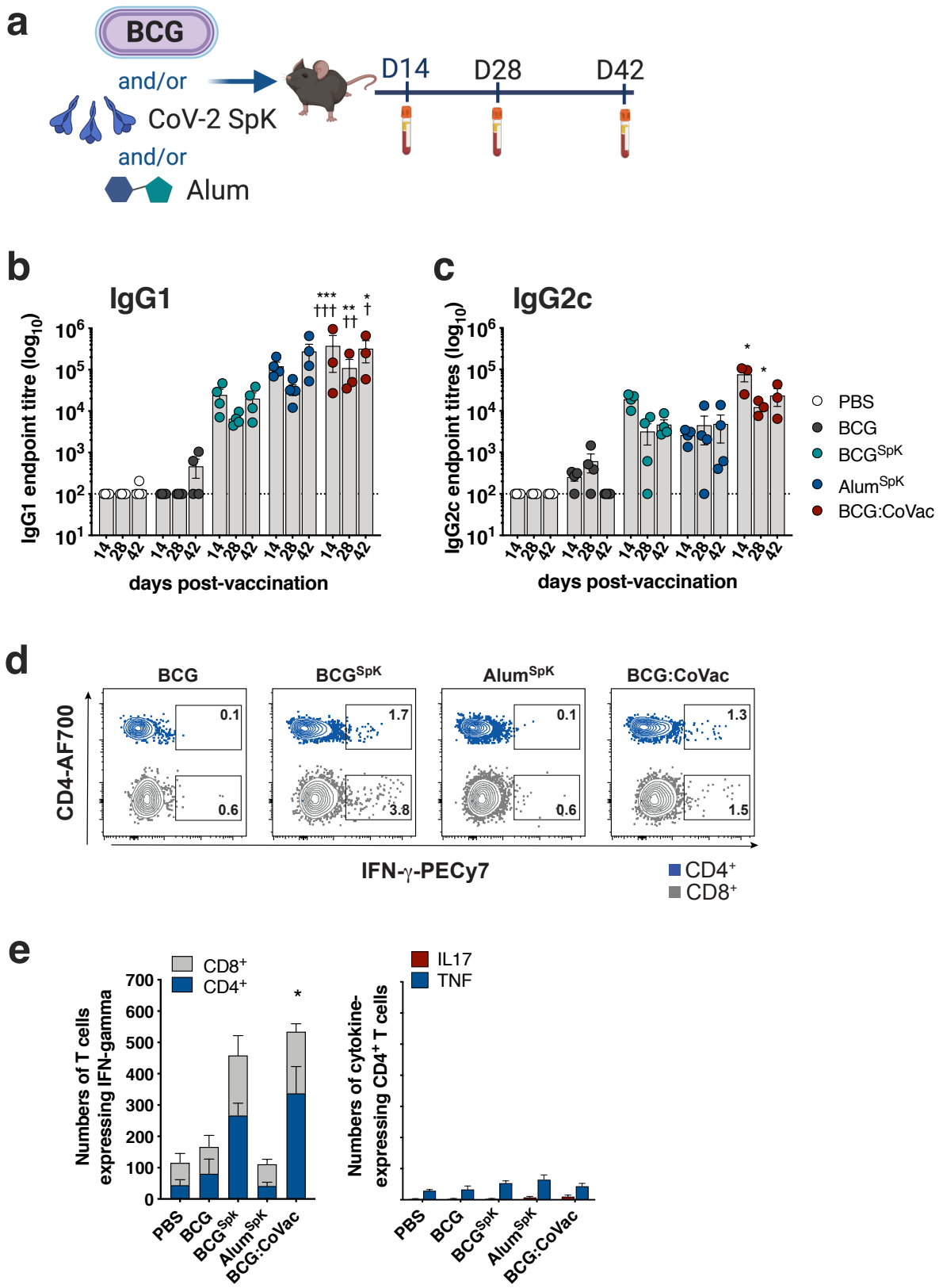
a
BCG
and/or
CoV-2 SpK
and/or
Alum
D14
D28
D42
b
IgG1
IgG1 endpoint titre (log10)
days post-vaccination
c
IgG2c
IgG2c endpoint titres (log10)
days post-vaccination
PBS
BCG
BCGSpK
AlumSpK
BCG:CoVac
d
BCG
BCGSpK
AlumSpK
BCG:CoVac
CD4-AF700
IFN-γ-PECy7
CD4+
CD8+
e
CD8+
CD4+
Numbers of T cells expressing IFN-gamma
IL17
TNF
Numbers of cytokine-expressing CD4+ T cells
PBS
BCG
BCGSpK
AlumSpK
BCG:CoVac

Figure 2

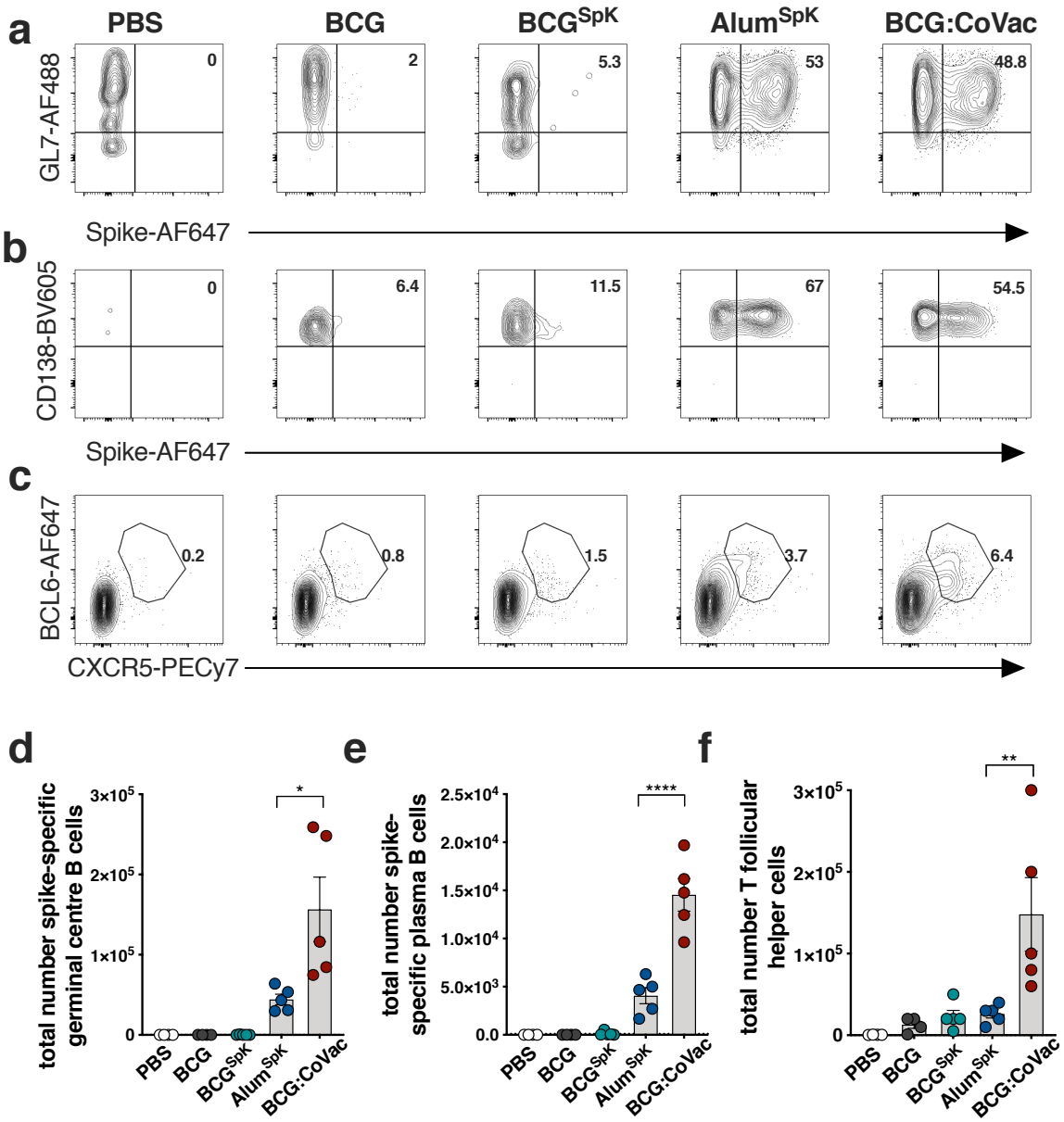

621
622
623
624
625
626
627
628
629

Figure 3

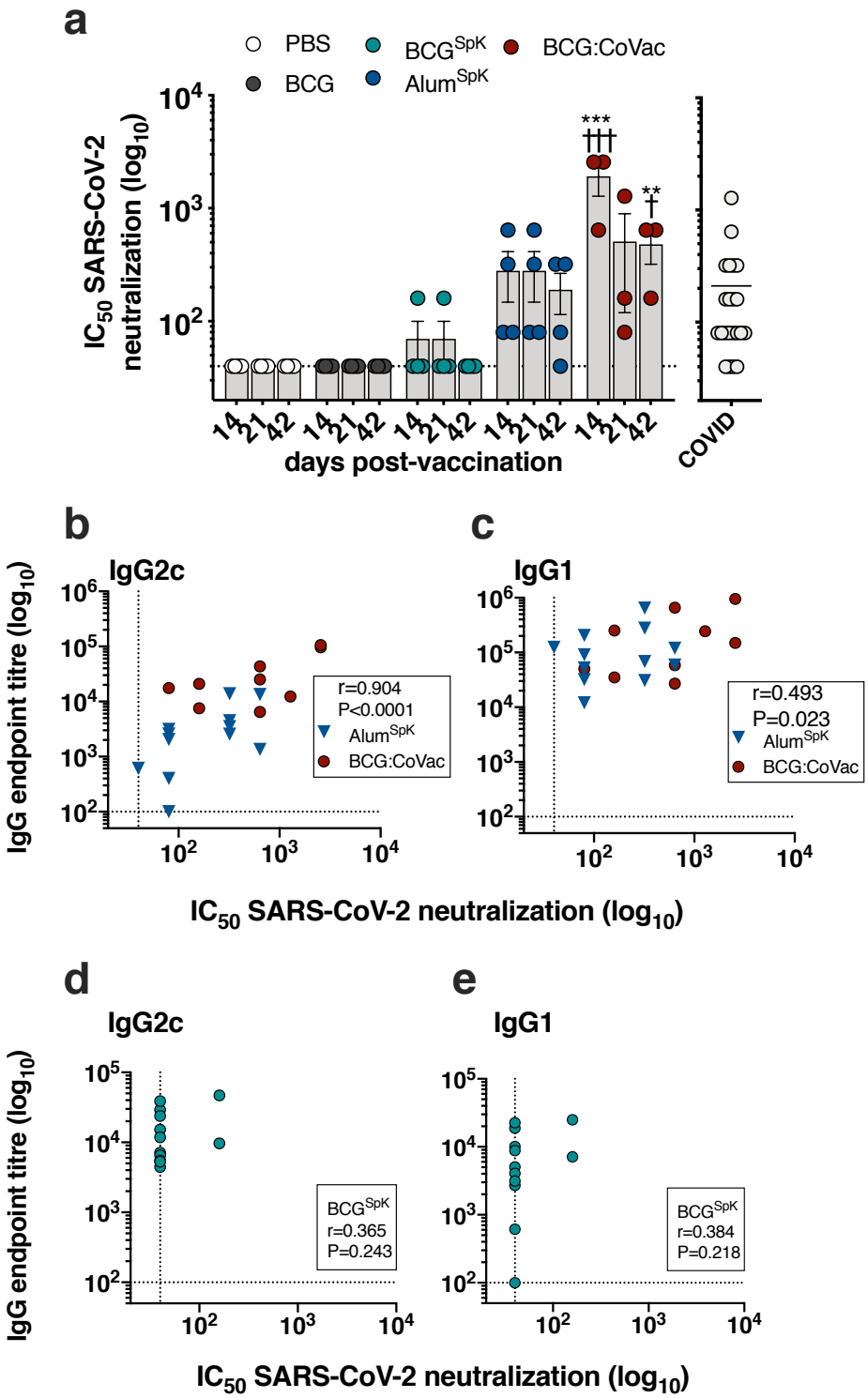
a
PBS
BCG
BCG^SpK
Alum^SpK
BCG:CoVac
IC50 SARS-CoV-2 neutralization (log10)
days post-vaccination
COVID
b
IgG2c
IgG endpoint titre (log10)
r=0.904
P<0.0001
Alum^SpK
BCG:CoVac
c
IgG1
r=0.493
P=0.023
Alum^SpK
BCG:CoVac
IC50 SARS-CoV-2 neutralization (log10)
d
IgG2c
IgG endpoint titre (log10)
BCG^SpK
r=0.365
P=0.243
e
IgG1
BCG^SpK
r=0.384
P=0.218
IC50 SARS-CoV-2 neutralization (log10)

Figure 4

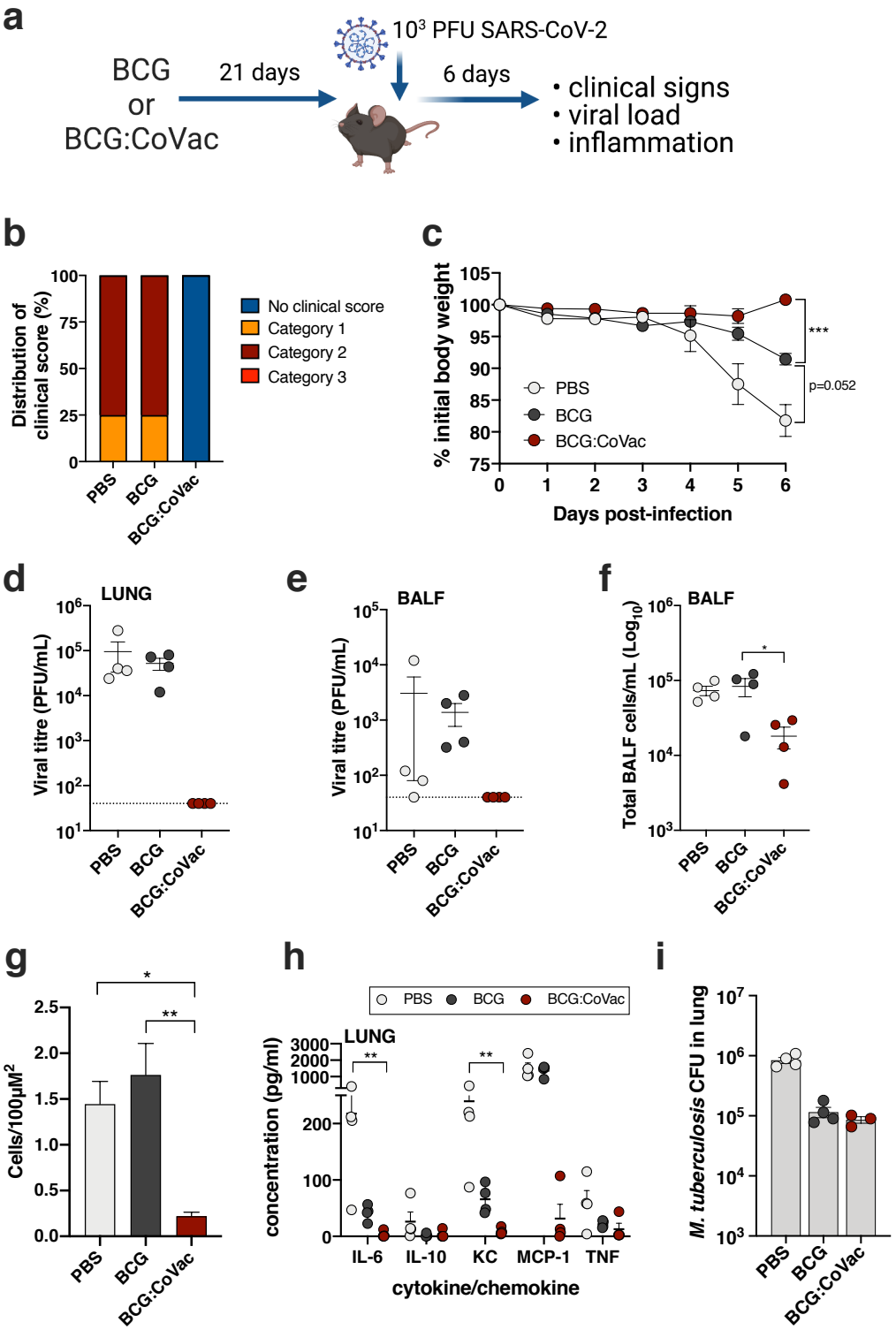

634

635

Figure 5

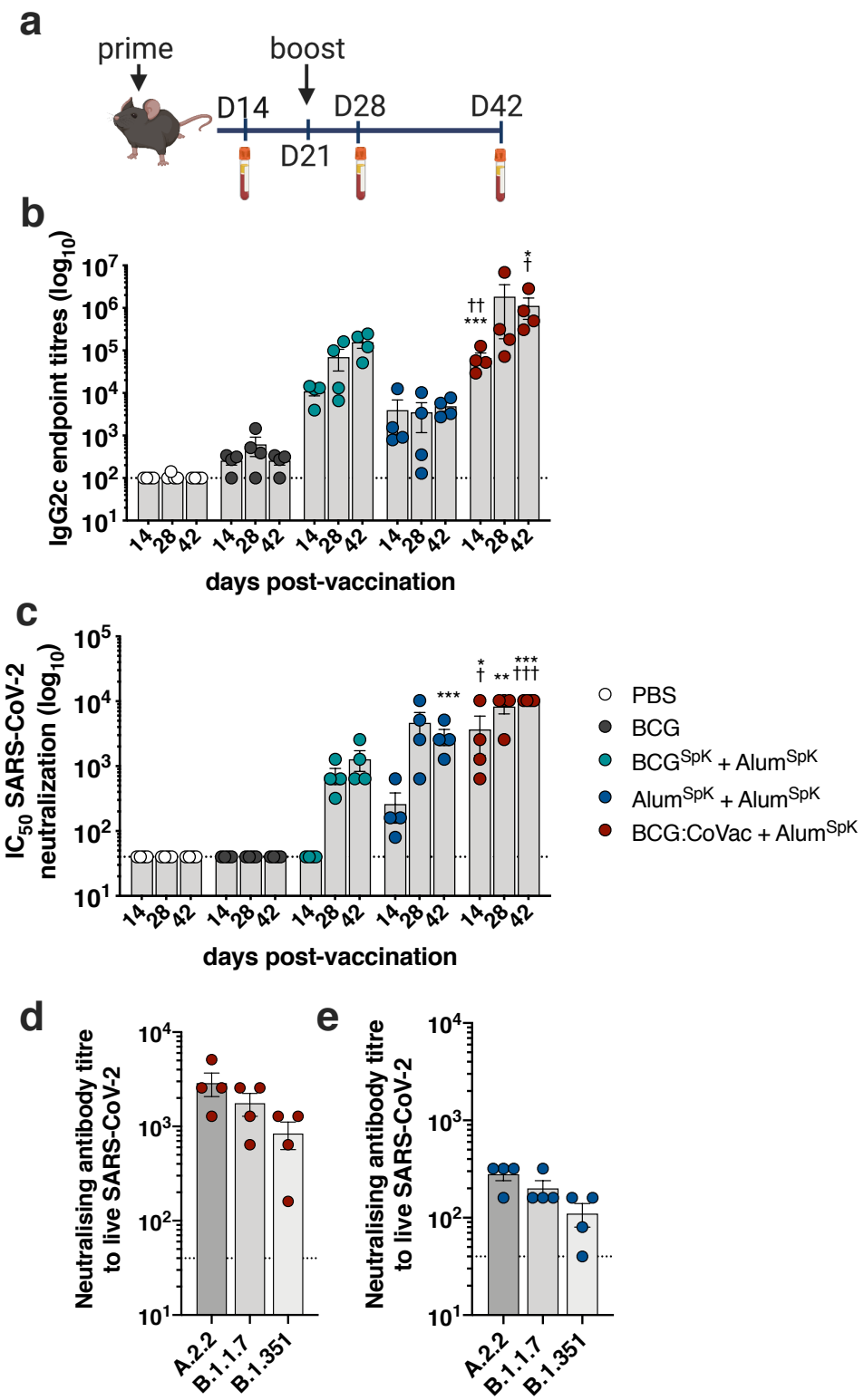

636

637

638

Figure S1

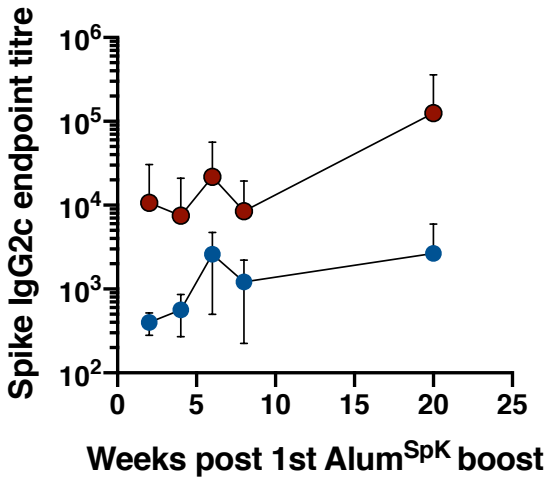

Fig. S1 | BCG promotes spike-specifica antibody reponses. Mice were vaccinated s.c with BCG ($5x10^5$ CFU) and 12 week later were vaccinated twice, 3 weeks apart with s.c with SARS-CoV-2 spike protein (5 μg) formulated in alum (100 μg; Alum^{SpK}). At the indicated timepoints the titre of spike-specific IgG2c in sera was determined by ELISA.

639
640
641
642
643
644
645
646
647
648
649

Figure S2

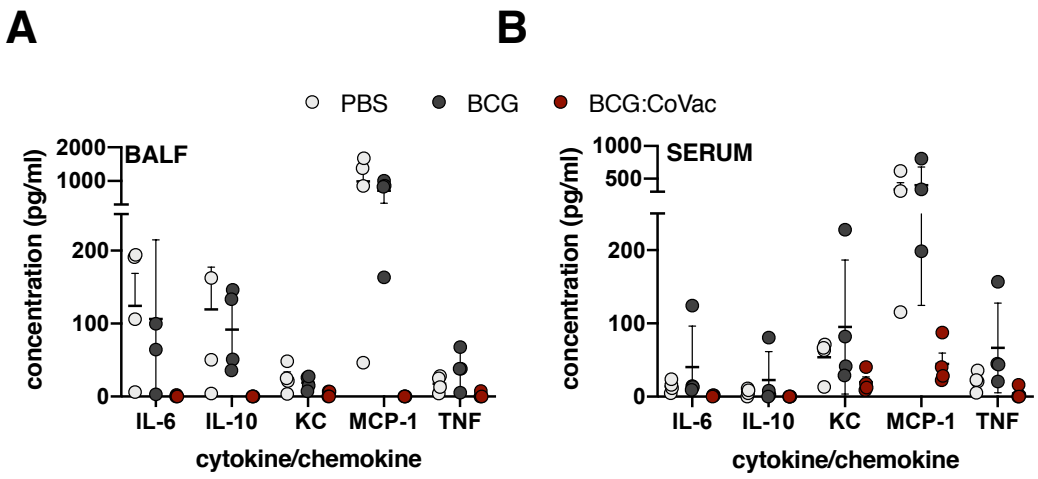

Fig. S2 | Single dose BCG:CoVac prevents the development of clinical disease in SARS-CoV-2 infected K18-hACE2 mice. a, Mice were immunised with sham (PBS), BCG or BCG:CoVac 21 days prior to challenge with 10^3 PFU SARS-CoV-2. Cytokine/chemokine levels were determined in BALF (**a**) and serum (**b**) by cytometric bead array.

650